Peer-reviewed version available at Mathematics 2020, 8, 1076; doi:10.3390/math8071076

Dynamics of periodic waves in a neural field model

N. Bessonov[1], **A. Beuter**[2,3], **S. Trofimchuk**[4], **V. Volpert**[5,6,7]

[1] Institute of Problems of Mechanical Engineering, Russian Academy of Sciences
199178 Saint Petersburg, Russia
[2] Bordeaux INP, Bordeaux, France; [3] CorStim SAS, Montpellier, France
[4] Instituto de Matematica y Fisica, Universidad de Talca, Casilla 747, Talca, Chile
[5] Institut Camille Jordan, UMR 5208 CNRS, University Lyon 1, 69622 Villeurbanne, France
[6] INRIA Team Dracula, INRIA Lyon La Doua, 69603 Villeurbanne, France
[7] Peoples Friendship University of Russia (RUDN University)
6 Miklukho-Maklaya St, Moscow, 117198, Russia

Abstract. Periodic travelling waves are observed in various brain activities including visual, motor, language, sleep, and so on. There are several neural field models describing periodic waves assuming nonlocal interaction and, possibly, inhibition, time delay, or some other properties. In this work we study the influence of asymmetric connectivity functions and of time delay on the emergence of periodic waves and on their properties. Nonlinear wave dynamics is studied, including modulated and aperiodic waves. Multiplicity of waves for the same values of parameters is observed. External stimulation in order to restore wave propagation in a damaged tissue is discussed.

Key words: neural field model, integro-differential equation, waves, brain stimulation

1 Introduction

1.1 Brain activity and periodic travelling waves

The brain displays a variety of highly nonlinear complex dynamics across multiple spatial and temporal scales [1]. About $86 \cdot 10^9$ neurons of the human brain entertain complex and fluctuating interactions. Understanding the dynamics of these interactions and the mechanisms underlying their control remains a technical and theoretical challenge. In other words, when healthy brain processes evolve toward abnormal and pathological states as a result of disease, degeneration or traumatic injury, how can a therapeutic intervention be used to reposition the control parameters and guide the dynamics back toward a healthy state? These brain processes are described today as interacting networks of nodes/hubs and edges which for the whole brain constitute the human connectome [3]. While the connectome is

focused on anatomical connections, the dynamics of the networks is represented by functional connections (also called the dynome [1]). For example, brain functional connections described as a graph explore how signals are transmitted along neuroanatomical pathways and interact with local dynamics. Functional connections are often investigated via modeling [1]. One possibility is to use mathematical models to identify how an outside intervention such as brain electrical stimulation can modify local dynamics and how local dynamics will in turn affect other brain regions.

Cortical brain dynamics are investigated via traveling waves (TW). A periodic traveling wave (TW) is defined as an oscillatory solution moving with constant shape and speed and which is periodic as a function of time and space. Cortical fibres project over long distances across the cortex, they provide the substrate for TW and govern their amplitude decay [5]. Propagating waves have been observed during almost every type of cortical processing examined. They provide subthreshold depolarization to individual neurons and increase their spiking probability. According to Muller et al. (2018), TW "travel over spatial scales that range from the mesoscopic (single cortical areas and millimetres of cortex) to the macroscopic (global patterns of activity over several centimeters) and extend over temporal scales from tens to hundreds of milliseconds". It has been proposed that TW mediate information transfer in the cortex.

In a review paper, the authors in [26] examined propagating waves of activity within and between cortical areas during action, perception or cognition. These authors suggest that TW are a manifestation of depolarization of the neuronal membrane of about 5 to 10 mV from resting potential, but this mild depolarization increases the probability of firing action potentials in the population and these spikes will in turn depolarize more postsynaptic neurons in the neighboring area to sustain the propagation of the TW [26]. But TW appear to subserve other functions as well. These authors suggest that a sensory-evoked wave propagating to a larger area would increase the sensitivity/network gain for incoming stimulation. In this sense, the evoked wave generates an unintentional focus of attention in the sensory cortex. Furthermore, propagating waves associated with an oscillation can organize spatial phase distributions in a population of neurons. In this context time delays play an important role in the unfolding of these TW.

In a more recent review [5] it was noted that cortical TW recorded at mesoscopic or macroscopic scales can be "spontaneously generated by recurrent circuits or evoked by external stimuli and travel along brain networks at multiple scales, transiently modulating spiking and excitability as they pass". The phase relation between oscillations in different cortical regions produce the TW and depending on the distance, axonal conduction delays can reach up to tens of milliseconds. These authors suggest that TW link high precision information with information from a broader contextual content and propagate over multiple functional regions, in the direction of maximum information transfer (some kind of gain adjustment).

Zhang et al. [4] examined direct brain recordings (ECoG) from neurosurgical patients performing a memory task and observed contiguous clusters of cortex in individual patients with oscillations at specific frequencies within 2 to 15 Hz. These oscillatory clusters displayed

spatial phase gradients, indicating that they formed traveling waves that propagated at about 0.25-0.75 m/s. These TW correlate with the subjects performance, propagate in specific directions and synchronize distributed cortical networks that are communicating. In other words, they guide the spatial propagation of neural activity demonstrating that large scale spatially coordinated oscillations, such as TW, figured prominently in human cortical processing.

Examining slow wave cortical activity during sleep-awake states using simultaneous scalp EEG and intracranial recordings in human subjects Botella-Soler et al. [28] identified for each subject the set of intracranial contacts that showed a larger percentage of detected events. They called these contacts "hubs" because the slow wave events in their travel through the cortical networks seemed to have a great probability of passing through the region close to the contact. Using probabilities they were able to reconstruct a preferential propagation network for each subject. Slow waves have been reported to propagate across cortical areas at about 1m/s with multiple propagation paths and several points of origin. It seems that the slow waves have a preference to start in the prefrontal cortex and to end in posterior and temporal regions of the cortex. These waves appear to shape and strengthen neuronal networks.

Let us also note that time delays are intrinsic to the dynamics of brain networks, nodes and edges. Propagation speed along axons depends on axonal length and diameter. Conduction times along neural circuits also depend on degree of fiber myelination. The introduction of time delays in models can lead to significant changes in brain dynamics. They can be averaged or treated as distributed delays. In this paper we address the question the effect of these delays in the dynamics of periodic cortical waves.

Thus, according to the biological observations, TW propagate in the cortex activating and coordinating different parts of the brain. In this work we will study some of their properties. In the next section, we will introduce the model. Then we present stability analysis which determines the conditions of wave appearance. Their nonlinear dynamics will be discussed in Section 3.

1.2 Neural field model

Neural field models were first introduced in [25]. Periodic travelling waves are described by several models (see [15, 18, 19, 20, 22] and Appendix 1). In this work we will consider one equation model with delay, and we will discuss two mechanisms of the emergence of such waves, which were not sufficiently investigated previously. The first mechanism is related to the asymmetric connectivity functions [14], and the second one is determined by the delay in the response function. It is known, that the loss of stability of the homogeneous in space solution in this model does not lead to the bifurcation of periodic waves [15]. We show that they still appear for some larger values of time delay. We consider the neural field equation for the electric potential in the brain cortex written in the form

$$\frac{\partial u}{\partial t} = D\frac{\partial^2 u}{\partial x^2} + W_a - W_i - \sigma u, \tag{1.1}$$

where W_a and W_i are the activating and inhibiting signals, respectively:

$$W_a(x,t) = \int_{-\infty}^{\infty} \phi_a(x-y) S_a\left(u\left(y, t - \frac{|x-y|}{q_a} - \tau_a\right)\right) dy, \tag{1.2}$$

$$W_i(x,t) = \int_{-\infty}^{\infty} \phi_i(x-y) S_i\left(u\left(y, t - \frac{|x-y|}{q_i} - \tau_i\right)\right) dy. \tag{1.3}$$

These expressions describe the intensity of signal coming from all points y to the point x. Here $S_a(u)$ and $S_i(u)$ are the excitation and inhibition response functions produced by activating (inhibitory) neurons, q_a are q_i is the excitation speeds, $|x-y|/q_{a,i}$ is the time delay due to the excitation propagation from the point y to the point x, $\phi_a(x,y)$ and $\phi_i(x,y)$ are the connectivity functions,

$$\phi_a(r) = \begin{cases} a_1 e^{-b_1 r} & , \quad r > 0 \\ a_3 e^{b_3 r} & , \quad r < 0 \end{cases}, \quad \phi_i(x) = \begin{cases} a_2 e^{-b_2 r} & , \quad r > 0 \\ a_4 e^{b_4 r} & , \quad r < 0 \end{cases}, \tag{1.4}$$

where a_i, b_i are some positive constants. Response functions $S_a(u)$ and $S_i(u)$ are non-negative non-decreasing functions usually considered as sigmoid functions. The last term in the right-hand side of equation (1.1) describes signal decay.

Neural field models are often considered without the diffusion term [13, 14, 11, 12]. From the mathematical point of view, introduction of the diffusion term is a generalization where the particular case $D = 0$ reduces it to the previous model. In [7] we showed that diffusion term influences the speed of wave propagation. In fact, there are two different regimes determined, respectively, by diffusion and by nonlocal interaction (connectivity function). The integral term in equation (1.1) describes signal transmission between neurons along the axons. There are other possible mechanisms which can influence neuron activation. The first one is ion diffusion through the extracellular matrix which changes the distribution of electric potential and influences neuron activity. Assuming that the latter is proportional to the ionic concentrations, we naturally describe it by the diffusion term. Similar action can be produced by gap junction communication where neurons (and possibly glia cells) exchange ions directly and not through the extracellular matrix. Finally, another mechanism is related to the ephaptic effect [10] where neurons feel electric gradients from large groups of activated neurons through the extracellular matrix and respond to them. Diffusion term suggests a phenomenological description of this effect taking into account space transmission of neuron activation "from large to small" values.

The speeds q_a, q_i of electric impulse propagation along axons is of the order 2-4 m/s while the speed of wave propagation is one-two orders of magnitude less [16] (p. 213). So, we will consider a large speed limit $q_a = q_i = \infty$:

$$\frac{\partial u}{\partial t} = D\frac{\partial^2 u}{\partial x^2} + \int_{-\infty}^{\infty} \left(\phi_a(x-y) S_a\left(u\left(y, t-\tau_a\right)\right) dy - \phi_i(x-y) S_i\left(u\left(y, t-\tau_i\right)\right)\right) dy - \sigma u. \tag{1.5}$$

Up to the diffusion term, which is not very essential for small diffusion coefficients, this model is a particular case of the two equation model considered in [15]. If the kernels in the two equations are the same, then the system can be reduced to the single equation.

Different neural field models describe propagation of periodic travelling waves (see Appendix 1). In this work we will consider two other mechanisms of their emergence. One of them is related to asymmetric kernels ϕ_a and ϕ_i whose existence is confirmed by the experimental observations [14]. Another one is determined by the secondary bifurcation. Similar to [15], we observe that the loss of stability of the homogeneous in space stationary solution leads to the appearance of periodic time oscillations independent of the space variable or of stationary periodic in space solutions. Periodic travelling waves bifurcate in the instability region, and they are unstable close to the bifurcation point. We will see that they can become stable under further change of parameters.

We will study dynamics of the periodic waves including their non-uniqueness for the same values of parameters. This property seems to us important since different waves $(\alpha, \beta, \gamma, \theta)$ are observed in the same brain.

2 Stability

2.1 Linearization and eigenvalues

In this section we will consider the equation

$$\frac{\partial u}{\partial t} = D\frac{\partial^2 u}{\partial x^2} + \int_{-\infty}^{\infty} \phi_a(x-y) S_a\left(u\left(y, t-\tau_a\right)\right) dy - \int_{-\infty}^{\infty} \phi_i(x-y) S_i\left(u\left(y, t-\tau_i\right)\right) dy - \sigma u, \quad (2.1)$$

on the interval $0 < x < L$ with periodic boundary conditions. We extend the function $u(x,t)$ by periodicity on the whole axis, $-\infty < x < \infty$, so that the integrals in equation (2.1) are well defined. Let u_0 be a solution of the equation

$$\phi_a^* S_a(u) + \phi_i^* S_i(u) - \sigma u = 0,$$

where $\phi_a^* = \int_{-\infty}^{\infty} \phi_a(x)dx$, $\phi_i^* = \int_{-\infty}^{\infty} \phi_i(x)dx$. Then u_0 is a stationary solution of equation (2.1). Linearizing this equation about u_0, we obtain the eigenvalue problem:

$$Dv'' + S_a'(u_0)e^{-\lambda\tau_a} \int_{-\infty}^{\infty} \phi_a(x-y)v(y)dy - S_i'(u_0)e^{-\lambda\tau_i} \int_{-\infty}^{\infty} \phi_i(x-y)v(y)dy - \sigma v = \lambda v. \quad (2.2)$$

Applying the Fourier transform, we get

$$S_a'(u_0)e^{-\lambda\tau_a}\tilde{\phi}_a(\xi) - S_i'(u_0)e^{-\lambda\tau_i}\tilde{\phi}_i(\xi) - D\xi^2 - \sigma = \lambda, \quad (2.3)$$

where

Peer-reviewed version available at Mathematics 2020, 8, 1076; doi:10.3390/math8071076

$$\tilde{\phi}_a(\xi) = \frac{a_1 b_1}{b_1^2+\xi^2} + \frac{a_3 b_3}{b_3^2+\xi^2} + i\xi\left(\frac{a_1}{b_1^2+\xi^2} - \frac{a_3}{b_3^2+\xi^2}\right),$$

$$\tilde{\phi}_i(\xi) = \frac{a_2 b_2}{b_2^2+\xi^2} + \frac{a_4 b_4}{b_4^2+\xi^2} + i\xi\left(\frac{a_2}{b_2^2+\xi^2} - \frac{a_4}{b_4^2+\xi^2}\right).$$

Set $\lambda = i\nu$. Separating the real and imaginary parts in equation (2.3), we obtain:

$$S_a'(u_0)\cos(\nu\tau_a)\left(\frac{a_1 b_1}{b_1^2+\xi^2} + \frac{a_3 b_3}{b_3^2+\xi^2}\right) + S_a'(u_0)\xi\sin(\nu\tau_a)\left(\frac{a_1}{b_1^2+\xi^2} - \frac{a_3}{b_3^2+\xi^2}\right) - \tag{2.4}$$
$$S_i'(u_0)\cos(\nu\tau_i)\left(\frac{a_2 b_2}{b_2^2+\xi^2} + \frac{a_4 b_4}{b_4^2+\xi^2}\right) - S_i'(u_0)\xi\sin(\nu\tau_i)\left(\frac{a_2}{b_2^2+\xi^2} - \frac{a_4}{b_4^2+\xi^2}\right) - D\xi^2 = \sigma,$$

$$-S_a'(u_0)\sin(\nu\tau_a)\left(\frac{a_1 b_1}{b_1^2+\xi^2} + \frac{a_3 b_3}{b_3^2+\xi^2}\right) + S_a'(u_0)\xi\cos(\nu\tau_a)\left(\frac{a_1}{b_1^2+\xi^2} - \frac{a_3}{b_3^2+\xi^2}\right) + \tag{2.5}$$
$$S_i'(u_0)\sin(\nu\tau_i)\left(\frac{a_2 b_2}{b_2^2+\xi^2} + \frac{a_4 b_4}{b_4^2+\xi^2}\right) - S_i'(u_0)\xi\cos(\nu\tau_i)\left(\frac{a_2}{b_2^2+\xi^2} - \frac{a_4}{b_4^2+\xi^2}\right) = \nu.$$

2.2 Symmetric connectivity functions with time delay

If the symmetry condition

$$a_1 = a_3, a_2 = a_4, b_1 = b_3, b_2 = b_4 \tag{2.6}$$

is satisfied, then equations (2.4), (2.5) write as follows:

$$S_a'(u_0)\cos(\nu\tau_a)\frac{a_1 b_1}{b_1^2+\xi^2} - S_i'(u_0)\cos(\nu\tau_i)\frac{a_2 b_2}{b_2^2+\xi^2} - D\xi^2/2 = \sigma/2, \tag{2.7}$$

$$-S_a'(u_0)\sin(\nu\tau_a)\frac{a_1 b_1}{b_1^2+\xi^2} + S_i'(u_0)\sin(\nu\tau_i)\frac{a_2 b_2}{b_2^2+\xi^2} = \nu/2. \tag{2.8}$$

We can express ξ^2 through ν from the last equation and substitute into equation (2.7). The resulting equation with respect to ν should be solved numerically or asymptotically. Since the calculations are sufficiently complex, we will consider here a simplified case where $\tau_a = 0$. Numerical simulations show that periodic waves can exist in this case (Section 3). Our aim here is to analyze their bifurcations from the homogeneous in space solution. Assuming that $\nu \geq 0$, we also get the conjugate solution $-\nu$.

If $\tau_a = 0$, then equations (2.7), (2.8) write as follows:

$$S_a'(u_0)\frac{a_1 b_1}{b_1^2+\xi^2} - S_i'(u_0)\cos(\nu\tau_i)\frac{a_2 b_2}{b_2^2+\xi^2} - D\xi^2/2 = \sigma/2, \tag{2.9}$$

$$S_i'(u_0)\sin(\nu\tau_i)\frac{a_2 b_2}{b_2^2+\xi^2} = \nu/2. \tag{2.10}$$

Peer-reviewed version available at Mathematics 2020, 8, 1076; doi:10.3390/math8071076

By stability boundary we will understand here the value $\sigma = \sigma_0$ such that system (2.9), (2.10) does not have solutions for $\sigma > \sigma_0$, and it has at least one solution for $\sigma < \sigma_0$. This stability boundary σ_0 is uniquely defined and it can be negative.

Proposition 1. *At the stability boundary,* $\xi = 0$ *or* $\nu = 0$.

Proof. Consider equation (2.10) as equation with respect to ν for a fixed ξ. It has a solution $\nu \neq 0$ if and only if

$$2\tau_i S_i'(u_0)\frac{a_2 b_2}{b_2^2 + \xi^2} > 1. \tag{2.11}$$

Suppose that this condition is satisfied for some ξ_0, and denote by $\nu(\xi)$ solution of equation (2.10) in the vicinity of $\xi = \xi_0 > 0$, and $\nu_0 = \nu(\xi_0)$. Assume that the corresponding value σ_0 belongs to the stability boundary.

Taking into account equation (2.10), we can write equation (2.9) as follows:

$$2S_a'(u_0)\frac{a_1 b_1}{b_1^2 + \xi^2} - \nu\cot(\nu\tau_i) - D\xi^2 = \sigma, \tag{2.12}$$

Let ξ_1 be sufficiently close to ξ_0 such that condition (2.11) remains satisfied, and $\xi_1 < \xi_0$. If $\nu(\xi_0) < 2\pi/\tau_i$, then $\nu(\xi_1) > \nu(\xi_0)$. Therefore,

$$\nu(\xi_1)\cot(\nu(\xi_1)\tau_i) < \nu(\xi_0)\cot(\nu(\xi_0)\tau_i).$$

Set

$$F(\xi) = 2S_a'(u_0)\frac{a_1 b_1}{b_1^2 + \xi^2} - \nu(\xi)\cot(\nu(\xi)\tau_i) - D\xi^2.$$

Thus, $F(\xi_1) > F(\xi_0)$. Hence, $\sigma_0 = F(\xi_0)$ cannot belong to the stability boundary since $\sigma_1 = F(\xi_1) > \sigma_0$, and system (2.9), (2.10) has a solution for $\sigma = \sigma_1$. This contradiction shows that the inequality $\nu(\xi_0) < 2\pi/\tau_i$ cannot hold.

Let $2\pi/\tau_i < \nu(\xi_0) < 5\pi/(2\tau_i)$. Then there is another solution $\nu_1(\xi_0)$ of equation (2.10) such that $\pi/(2\tau_i) < \nu_1(\xi_0) < \pi/\tau_i$. Therefore, $cos(\nu_1(\xi_0)\tau_i) < 0$, $cos(\nu(\xi_0)\tau_i) > 0$, and

$$\sigma_0 = F(\xi_0) < 2S_a'(u_0)\frac{a_1 b_1}{b_1^2 + \xi_0^2} - \nu_1(\xi_0)\cot(\nu_1(\xi_0)\tau_i) - D\xi_0^2.$$

Hence, σ_0 cannot belong to the stability boundary.

Finally, in all other cases with $\nu(\xi_0) > 5\pi/(2\tau_i)$ we obtain a contradiction similarly to the two cases considered before. This contradiction shows that at the stability boundary, either $\xi = 0$ or $\nu = 0$.

□

Let us now determine the stability boundary with respect to time delay for a fixed σ. If $\nu = 0$, then from equation (2.9) we get

$$\sigma = \frac{\alpha_1}{b_1^2+\xi^2} - \frac{\alpha_2}{b_2^2+\xi^2} - D\xi^2, \tag{2.13}$$

where $\alpha_1 = 2S_a'(u_0)a_1b_1$, $\alpha_2 = 2S_i'(u_0)a_2b_2$. Assuming that $\nu \neq 0$, we set $\beta_i = \alpha_i/(b_i^2 + \xi^2)$, $i = 1, 2$. Then $sin(\nu\tau_i) = \nu/\beta_2$,

$$\beta_1 - \sqrt{\beta_2^2 - \nu^2} = \sigma, \quad \nu^2 = \beta_2^2 - (\beta_1 - \sigma)^2.$$

Example. Consider the values of parameters: $S_a'(u_0) = S_i'(u_0) = 20, a_1 = a_2 = 4, b_1 = 40, b_2 = 20, \alpha_1 = 6400, \alpha_2 = 3200$, $\sigma = 0.01$, Then we find

$$\xi = 0, \beta_1 = 4, \beta_2 = 8, \nu^2 \approx 48, \nu \approx 6.93, \quad \tau_i = \frac{1}{\nu}\arcsin\frac{\nu}{\beta_2} = 0.151,$$

and

$$\xi = \pi, \beta_1 = 3.975, \beta_2 = 7.805, \nu^2 \approx 45.123, \nu \approx 6.717, \quad \tau_i = \frac{1}{\nu}\arcsin\frac{\nu}{\beta_2} = 0.154$$

Hence, the homogeneous in space oscillations appear for a lesser value of time delay than periodic travelling waves. Therefore, these waves are unstable in the vicinity of the bifurcation point. We will see in the next section that they become stable for larger values of time delay.

2.3 Asymmetric connectivity function without time delay

Suppose now that conditions (2.6) are not satisfied. In this case, the eigenvalue (2.3) has a nonzero imaginary part. Set $\lambda(\xi) = \alpha(\xi) + i\beta(\xi)$, where

$$\alpha(\xi) = \frac{s_a a_1 b_1}{b_1^2+\xi^2} + \frac{s_a a_3 b_3}{b_3^2+\xi^2} - \frac{s_i a_2 b_2}{b_2^2+\xi^2} - \frac{s_i a_4 b_4}{b_4^2+\xi^2} - D\xi^2 - \sigma,$$

$$\beta(\xi) = s_a\xi\left(\frac{a_1}{b_1^2+\xi^2} - \frac{a_3}{b_3^2+\xi^2}\right) - s_i\xi\left(\frac{a_2}{b_2^2+\xi^2} - \frac{a_4}{b_4^2+\xi^2}\right), \tag{2.14}$$

$s_a = S_a'(u_0), s_i = S_i'(u_0)$. As before, the stability boundary is given by the condition $\alpha(\xi) = 0$:

$$\sigma = \frac{s_a a_1 b_1}{b_1^2+\xi^2} + \frac{s_a a_3 b_3}{b_3^2+\xi^2} - \frac{s_i a_2 b_2}{b_2^2+\xi^2} - \frac{s_i a_4 b_4}{b_4^2+\xi^2} - D\xi^2 \equiv \Phi_2(\xi). \tag{2.15}$$

The instability occurs if $\sigma < \Phi_2(\xi)$ for some values of ξ. Since there are two complex conjugate eigenvalues $\lambda(\xi) = \alpha(\xi) \pm i\beta(\xi)$, then at the stability boundary $\alpha = 0$ the bounded solution of the linearized equation writes

$$u(x,t) = e^{i\beta t}e^{i\xi x} + e^{-i\beta t}e^{-i\xi x} = \cos(\beta t + \xi x).$$

Here ξ is found from the equation $\alpha(\xi) = 0$ and β is given by equality (2.14). This solution represents a periodic wave with frequency ξ and speed $c = -\beta/\xi$. We get from (2.14):

$$c = -s_a \left(\frac{a_1}{b_1^2 + \xi^2} - \frac{a_3}{b_3^2 + \xi^2} \right) + s_i \left(\frac{a_2}{b_2^2 + \xi^2} - \frac{a_4}{b_4^2 + \xi^2} \right) \tag{2.16}$$

If there are two (or more) different frequencies ξ_1 and ξ_2 satisfying the condition $\sigma < \Phi(\xi_j)$, $j = 1, 2$, then there are two waves with different speeds and frequencies. According to (2.16), the value of the speed can increase with frequency or decrease depending on the values of parameters.

3 Numerical simulations

In this section we present the results of numerical simulations of equation (2.1) on a bounded interval with periodic boundary conditions. We begin with the case without time delay and continue with the case of time delay in the response functions. We will finish this section with modelling of the stimulation of the damaged tissue in order to restore wave propagation.

3.1 Wave propagation without time delay

In the case without time delay ($\tau_a = \tau_i = 0$) and with symmetric connectivity functions ϕ_a and ϕ_i, where $a_1 = a_3, a_2 = a_4, b_1 = b_3, b_2 = b_4$, the homogeneous in space stationary solution can lose its stability resulting in appearance of periodic in space stationary solutions. Linear stability analysis shows that travelling waves with nonzero speed do not bifurcate in this case.

If the connectivity functions are not symmetric, then travelling waves with nonzero speed are observed. Two types of solutions are observed in numerical simulations: periodic waves with a constant speed and aperiodic waves with oscillating speed. In the first case, the wave has conventional form $w(x - ct)$, where $w(x)$ is a periodic in space function and c is a constant (Figure 1, left). In the second case, the amplitude of spatial peaks and the wave speed oscillate (Figure 1, right).

Different periodic regimes can co-exist for the same values of parameters. Figure 2 shows the dependence of the wave speed on the values $a_1 (= a_2)$ for all other parameters fixed. There are three branches of solutions corresponding to different spatial frequencies. Thus, there are three different periodic waves for the same values of parameters with the speeds depending on their frequency.

For a_1 sufficiently small, transition to modulated waves can occur (curve 1) with the amplitude and speed depending on time. These solutions can qualitatively approximated as $u(x,t) = (a + \epsilon \sin(b_1 x + c_1 t)) \sin(b_2 x + c_2 t)$, where a, b_1, b_2, c_1, c_2 are some constants. For even lesser values of a_1 transition to aperiodic oscillations is observed for all three branches of solutions. These oscillations can coexist with periodic or modulated periodic waves for the same values of parameters.

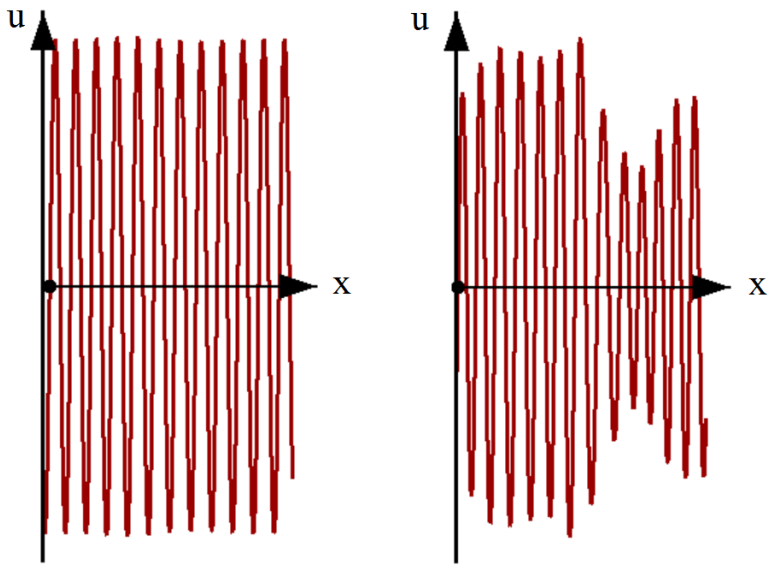

Figure 1: Wave propagation described by equation (2.1) for $\tau_a = \tau_i = 0$. Periodic (left) and aperiodic (right) waves can exist for the same values of parameters. Convergence of solutions to one of them is determined by the initial conditions. The values of parameters are as follows: $a_1 = a_2 = 0.6, a_3 = a_4 = 4$, $b_1 = b_3 = 40, b_2 = b_4 = 20$, $D = 10^{-4}$, $\sigma = 0.01$, $S_a(u) = S_i(u) = \arctan(hu)$, $h = 20$, $L = 2$.

3.2 Time delay and symmetric connectivity functions

Initial conditions. As it was discussed in the previous section, the loss of stability of the homogeneous in space stationary solution leads either to the homogeneous in space time oscillations or to the stationary periodic in space solutions. Consider time delay as a bifurcation parameters. If it exceed a critical value, then time oscillations emerge. Periodic travelling waves bifurcate for a larger value of time delay, and they are unstable in the vicinity of the bifurcation point. Numerical simulations show that they can become stable under further increase of τ. Nevertheless, periodic time oscillations homogeneous in space remain stable. Therefore, we need to choose some particular initial conditions in order to get periodic travelling waves.

The simulations presented in this section are carried out with two types of initial conditions. In the first case, we consider the equation

$$\frac{\partial u}{\partial t} = D\frac{\partial^2 u}{\partial x^2} + I(x,t) \tag{3.1}$$

on the time interval $0 \le t \le T_0$. Here $I(x,t) = I_0 \cos(px + qt)$, and the initial condition $u(x,0) = 0$. The result of this simulation is considered as initial condition for equation (1.5). We set $I_0 = 0.5, q = 0.015, T_0 = 20$, the value of p is taken $3, 6, 9$ depending on the required space periodicity.

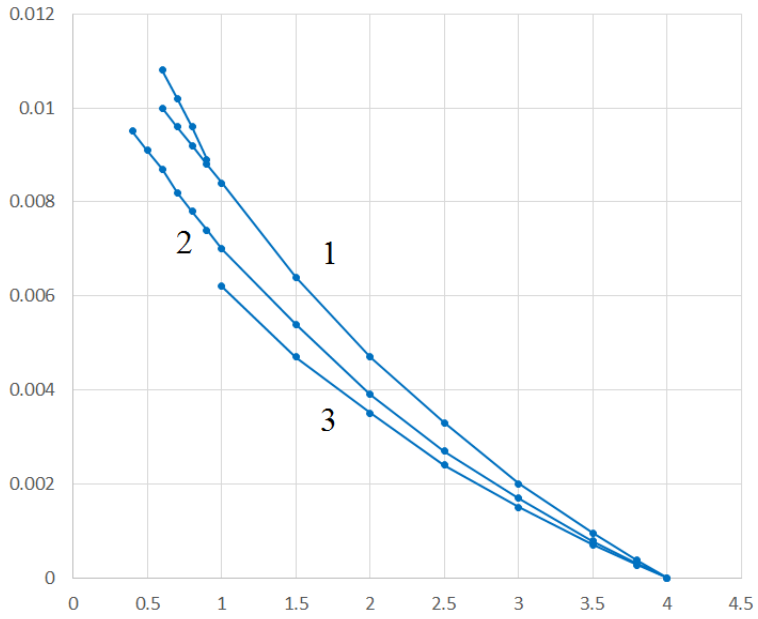

Figure 2: The speed of periodic waves for different values of the parameters $a_1 = a_2$. Three curves correspond to different values of the spatial frequency: 1. 12 periods of solution, 2. 13 periods, 3. 14 periods. Branching in curve 1 shows the transition to modulated oscillations with the maximal and minimal values of the oscillating speed. The values of parameters are as follows: $a_3 = a_4 = 4$, $b_1 = b_3 = 40, b_2 = b_4 = 20$, $D = 10^{-4}$, $\sigma = 0.01$, $S_a(u) = S_i(u) = \arctan(hu)$, $h = 20$, $L = 2$.

The second type of initial conditions is used in the continuation method. The results of the simulations of equation (1.5) for some values of parameters are used as initial conditions for some other values of parameters.

Multiplicity of waves and parameter dependence. An example of periodic travelling waves with different initial conditions and the same values of parameters are shown in Figure 3. We observe one-, two-, and three-period waves observed for $p = 3, 6$, and 9 in the function $I(x, t)$. These waves have different speeds and amplitude (Figure 4). The waves with larger wavelength have larger speed and amplitude. Increase of time delay leads to the increase of the wave amplitude and to the decrease of its speed. If time delay is sufficiently small, then the waves become unstable, and the transition to the periodic time oscillations independent of the space variable is observed. If the value I_0 is small enough, then the solution converges to the homogeneous time oscillations.

Figure 5 shows the dependence of periodic waves on the value b_2 (equal to b_4). The wave amplitude and speed decrease with the increase of b_2. There is a critical value $b_2 \approx 40$ for which the speed becomes zero, and a transition to another branch of solutions is observed. These are stationary periodic in space solutions with growing amplitude as b_2 increases. It

Preprints (www.preprints.org) | NOT PEER-REVIEWED | Posted: 8 March 2020 doi:10.20944/preprints202003.0135.v1

Peer-reviewed version available at Mathematics 2020, 8, 1076; doi:10.3390/math8071076

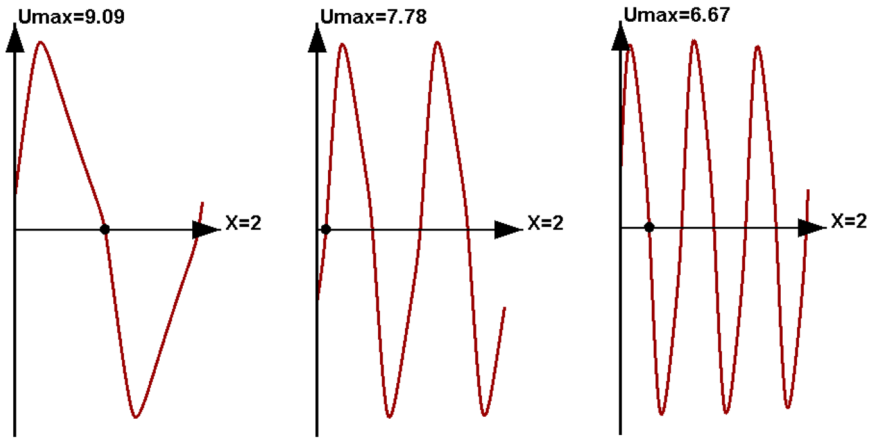

Figure 3: Three types of periodic waves observed for the same values of parameters and having different spatial frequency and speed: one-period wave with speed -0.027 (left); two-period wave with speed -0.012 (middle); three-period wave with speed -0.0094. The values of parameters are as follows: $\tau_a = 0, \tau_i = 12$, $a_1 = a_2 = a_3 = a_4 = 4$, $b_1 = b_3 = 40, b_2 = b_4 = 20$, $D = 10^{-4}$, $\sigma = 0.01$, $S_a(u) = S_i(u) = \arctan(hu)$, $h = 20$, $L = 2$.

is interesting to note the existence of weakly oscillating time periodic solutions in a narrow interval between travelling waves and stationary solutions.

The results presented above are obtained for a single delay τ_i in the inhibition term while $\tau_a = 0$. If we fix $\tau_i = 1$ and increase τ_a beginning from $\tau_a = 0$, then the amplitude and the speed of travelling waves are not monotone. The former first decreases, passes through the minimum and then increases, while the latter increases in the beginning and decreases for larger values of the delay (not shown).

3.3 Stimulation

Exact solution of the stimulation problem. Signal propagation can be different in the normal and in the damaged tissues since their properties differ from each other. Let us write equation (2.1) for the normal tissue

$$\frac{\partial u}{\partial t} = D\frac{\partial^2 u}{\partial x^2} + J(u) - \sigma u, \tag{3.2}$$

where

$$J(u) = \int_{-\infty}^{\infty} \phi_a(x-y) S_a\left(u\left(y, t-\tau_a\right)\right) dy - \int_{-\infty}^{\infty} \phi_i(x-y) S_i\left(u\left(y, t-\tau_i\right)\right) dy,$$

and a similar equation for the damaged tissue

$$\frac{\partial v}{\partial t} = D\frac{\partial^2 v}{\partial x^2} + J^*(v) - \sigma v, \tag{3.3}$$

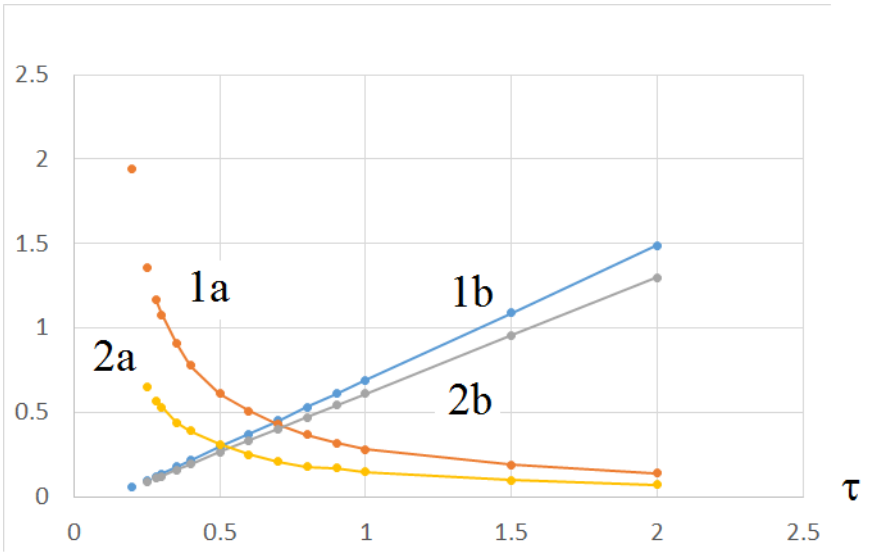

Figure 4: The speed (1a, 2a) and the amplitude (1b, 2b) for the one-period wave (1a, 1b) and two-period wave (2a, 2b) depending on τ_i. Connected points correspond to stable solutions, separate points to unstable solutions. The latter lead to the appearance of stationary solutions periodic in space. The values of parameters are as follows: $\tau_a = 0$, $a_1 = a_2 = a_3 = a_4 = 4$, $b_1 = b_3 = 40, b_2 = b_4 = 20$, $D = 10^{-4}$, $\sigma = 0.01$, $S_a(u) = S_i(u) = \arctan(hu)$, $h = 20$.

where

$$J^*(v) = \int_{-\infty}^{\infty} \phi_a^*(x-y) S_a^*\left(v\left(y, t-\tau_a\right)\right) dy - \int_{-\infty}^{\infty} \phi_i^*(x-y) S_i^*\left(v\left(y, t-\tau_i\right)\right) dy,$$

$\phi_{a,i}^*$, $S_{a,i}^*$ denote the connectivity and response functions for the damaged tissue. The solutions $u(x,t)$ and $v(x,t)$ can be different even if the initial conditions are the same, $u(x,0) = v(x,0)$ for $x \in \mathbb{R}$.

Consider, next, equation for the damaged tissue with an external stimulation $I(x,t)$:

$$\frac{\partial z}{\partial t} = D\frac{\partial^2 z}{\partial x^2} + J^*(z) - \sigma z + I(x,t). \tag{3.4}$$

We are interested whether it is possible to choose stimulation $I(x,t)$ in such a way that solution $z(x,t)$ of equation (3.4) becomes the same as solution $u(x,t)$ of equation (3.2). If this is possible, then external stimulation can completely reconstruct wave propagation. In spite of the importance of this problem for the application, the solution of this seemingly difficult question is simple. Assuming that $z(x,t) = u(x,t)$, substitute the function $u(x,t)$ in equation (3.4). Then we get

$$I(x,t) = \frac{\partial u}{\partial t} - D\frac{\partial^2 u}{\partial x^2} - J^*(u) + \sigma u = J(u) - J^*(u).$$

Preprints (www.preprints.org) | NOT PEER-REVIEWED | Posted: 8 March 2020 doi:10.20944/preprints202003.0135.v1

Peer-reviewed version available at Mathematics 2020, 8, 1076; doi:10.3390/math8071076

Thus, the stimulation function

$$I(x,t) = J(u) - J^*(u)$$

gives solution of the complete reconstruction problem.

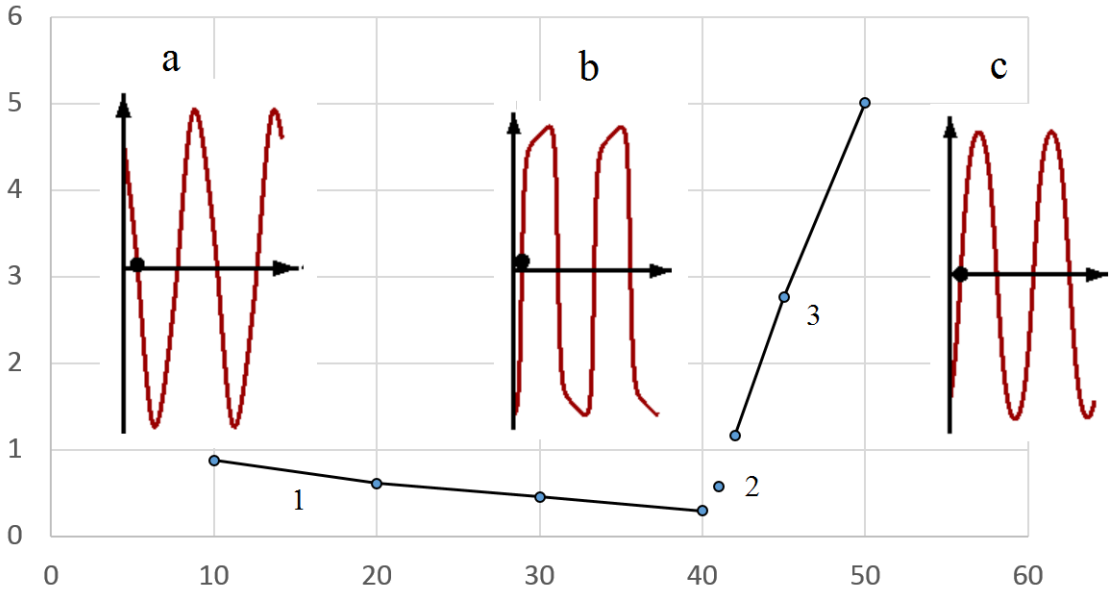

Figure 5: Dependence on $b_2(= b_4)$. Periodic travelling waves on branch 1 for $b_2 = 10$ (a) and $b_2 = 40$ (b); stationary solution on branch 3 for $b_2 = 50$ (c). A short branch 2 contains weakly oscillating solutions. The values of parameters are as follows: $\tau_a = 0, \tau_i = 1$, $a_1 = a_2 = a_3 = a_4 = 4$, $b_1 = b_3 = 40$, $D = 10^{-4}$, $\sigma = 0.01$, $S_a(u) = S_i(u) = \arctan(hu)$, $h = 20$, $L = 2$.

Approximate solution of the stimulation problem. Stimulation function suggested above uses the solution $u(x,t)$ which may not be known for the patient with the damaged brain tissue. In this case, some approximate solutions of the stimulation problem can be used. Consider the integral $J^*(v)$ in the following form:

$$J^*(v) = \int_{-\infty}^{\infty} W(x)W(y)\left(\phi_a(x-y)S_a\left(v\left(y,t-\tau_a\right)\right) - \phi_i(x-y)S_i\left(v\left(y,t-\tau_i\right)\right)\right)dy,$$

where $W(x) = w_0 < 1$ for $x_1 \le x \le x_2$, $x_1, x_2 \in (0, L)$, and $W(x) = 1$ outside the interval $[x_1, x_2]$. Hence, the connectivity function decreases if x or y belongs to the damaged area $[x_1, x_2]$. If we set $w_0 = 0$, then the connectivity function vanish if one of the two points x or y (neurons) belongs to the damaged area.

Without damage, periodic travelling wave solution of equation (3.2) and the integral $J(u)$ can be approximated by cosine function (Figure 6). Hence, we will look for the stimulation

Preprints (www.preprints.org) | NOT PEER-REVIEWED | Posted: 8 March 2020 doi:10.20944/preprints202003.0135.v1

Peer-reviewed version available at Mathematics 2020, 8, 1076; doi:10.3390/math8071076

function in the form approximating the periodic wave: $I(x,t) = I_0(x)\cos(px+qt)$. We $p = 6$, $q = 1$ to approximate the frequency and the speed of the wave in the normal tissue. We set $I_0(x) = i_0$ for $x_1 \le x \le x_2$, and $I_0(x) = i_1$ outside the interval $[x_1, x_2]$. The results of numerical simulations are presented in Figure 6 with the comparison of the normal tissue, damaged tissue without stimulation and damaged tissue with stimulation. We observe a periodic wave in the normal tissue. Behavior of solution is completely different in the damaged tissue. The solution is close to 0 at the damaged interval (green in the middle figure), and it oscillates periodically in time from both sides of this interval. Stimulation restores the wave propagation with the same frequency and speed. The choice of the stimulation amplitude $i_0 = 0.6$ and $i_1 = 0.1$ (for the example in the figure) is important. If we set $i_0 = 0.6, i_1 = 0$, the stimulation is not successful, there is no wave propagation. Thus, stimulation should be done not only inside the damaged interval but also around it.

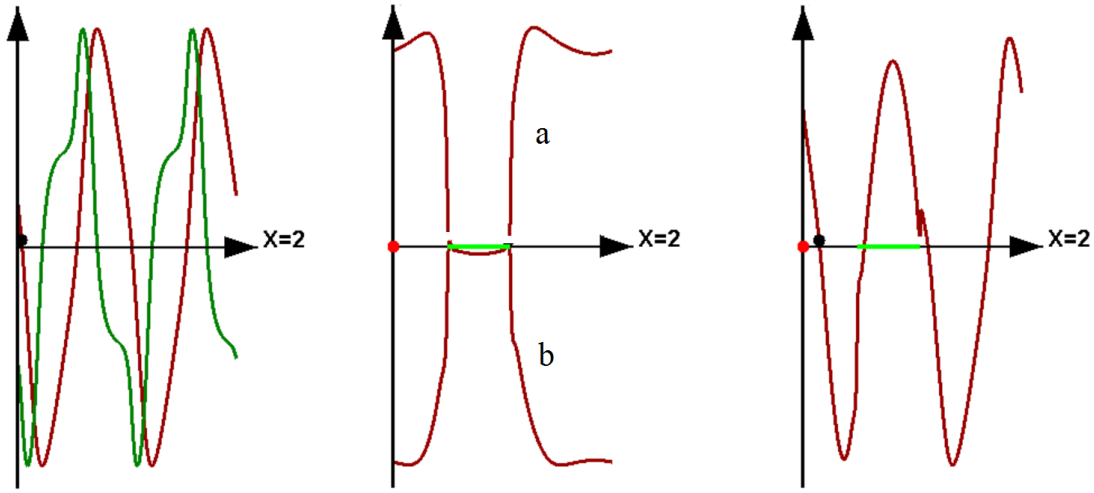

Figure 6: Periodic travelling wave in the normal tissue and the integral $J(u)$ (left). Snapshots of solutions in the damaged tissue for two different moments of time (a) and (b) (middle). Solution with stimulation becomes close to the periodic wave (right). The values of parameters are as follows: $\tau_a = 0, \tau_i = 1$, $a_1 = a_2 = a_3 = a_4 = 4$, $b_1 = b_3 = 40, b_2 = b_4 = 20$, $D = 10^{-4}$, $\sigma = 0.01$, $S_a(u) = S_i(u) = \arctan(hu)$, $h = 20$, $L = 2$, $p = 6, q = 1, i_0 = 0.6, i_1 = 0.1$. The damaged interval (green line) is $[0.5, 1.07]$, $w_0 = 0$.

4 Discussion

Brain functioning is determined by large scale networks of epicenters (hubs) located in the cortex and connected by white matter fiber tracks. The structure of these networks depends on the particular type of the brain activity (motor, language, and so on) and on the inter-individual variation. The epicenters exchange information by means of signaling along the

cortex or along the white matter fibers. Apparently, this signaling occurs in the form of travelling waves. Periodic travelling waves are observed in thalamus, visual cortex, hippocampus, and in other parts of the brain. There is more and more evidence that they play the key roles in brain functioning. However, their exact role and organization are not known. Their characteristics, such as speed, frequency, and amplitude can vary in wide limits (Appendix 2), and it is not clear how they are initiated and stop, and how they are related to some particular type of activities. For example, periodic waves are observed in the beginning of speaking, and they inverse their direction at the end [27]. The corresponding mechanisms governing these activities are not yet understood. These investigations are at the stage of accumulation of biological data and of elaboration of different models whose role and utility will become clearer with time.

Neural field models are widely used to study brain patterns, including stationary structures, pulses, wave fronts, and periodic waves. There is a number of models which describe periodic waves (Appendix 1) since it is relatively easy to find these waves on the basis of linear stability analysis of the homogeneous in space stationary solution. The mechanisms of this instability can be related to a combination of inhibition, time delay, refractoriness (also a variant of time delay), nonlocal interaction. In this work we study the influence of asymmetry of connectivity functions and of time delay in neuron response.

Neuron connectivity is provided by numerous axons whose density decrease approximately exponentially as a function of distance [23, 24]. In modelling, the connectivity functions are usually considered to be symmetric, that is, axon connections between points x and y have the same density as between y and x. There is some evidence that connectivity can be asymmetric [14].

Travelling waves in speech. Travelling waves in the cortex can have several functions including activation of some of its parts. This activation facilitates firing of individual neurons [26]. We conjecture that this can be a preparatory step for receiving the information from other brain areas along the white matter fibers.

TW have also been examined during speech. Rapela (2018) [27] examined direct brain recordings (ECoG) in neurosurgical patients producing consonant-vowel syllables (CVSs). The author showed that TWs do not occur continuously, but tend to appear before the initiation of CVSs and tend to disappear before their termination. During moments of silence, between productions of CVSs, TWs tend to reverse direction. Rapela observed a concentration of phase across trials at the specific frequency of speech production as well as amplitude modulation and phase-amplitude coupling (PAC). This study shows that TW induces an organization of PAC so that spiking occurs at behaviorally relevant times (i.e., TW across the left speech processing brain areas synchronized to the rhythm of speech production).

Summarizing results by Gross et al. [29] examining how brain waves help us make sense of speech in healthy subjects, Weaver [30] writes that speech consists of a hierarchy of components that each takes place on a different timescale. Speech cues such as intonation occur on a relatively long timescale, unfolding over hundreds of milliseconds. At the other

end of the spectrum is the phoneme the smallest unit of speech which lasts only tens of milliseconds. To understand speech efficiently necessitates simultaneous processing of different speech components occurring on various timescales. It was observed that neural oscillations were arranged in a hierarchy: "delta oscillations influenced the magnitude of theta oscillations, which in turn affected the amplitude of gamma oscillations".

Today, the language networks have been identified with precision. For example, Sarubbo et al. [31] summarize their observations in the following way: "The medial part of dorsal stream (arcuate fasciculus) subserves phonological processing; its lateral part [indirect anterior portion of the superior longitudinal fascicle (SLF)] subserves speech planning". The ventral stream subserves language semantics and matches with the inferior fronto-occipital fascicle. Reading deficits match with the inferior longitudinal fascicle. Anomias match with the indirect posterior portion of the SLF. Frontal WM underpins motor planning and execution. Right parietal WM subserves spatial cognition. Sensori-motor and visual fibers were the most preserved bundles.

Based on these observations what could be the role of cortical TW? We hypothesize that cortical TW reflect information originating from right and left hemispheres, traveling short and long distances, and containing various time delays. In other words TW coordinate multiple faster and slower speech events by preparing the arrival of signals traveling along white matter tracts to specific hubs. These observations open the possibility to combine information from language networks with information from the organization of cortical TW in order to design new cortical stimulation protocols in patients with language deficits.

Acknowledgments

The work was supported by the "RUDN University Program 5-100" and the French-Russian project PRC2307.

References

[1] N. Kopell, H. J. Gritton, M. A. Whittington, M. A. Kramer. Beyond The Connectome: The Dynome. Neuron. 2014 September 17; 83(6): 13191328. doi:10.1016/j.neuron.2014.08.016.

[2] G. Shepherd. Neurobiology, Oxford University Press, New York, 1994.

[3] O. Sporns. The human connectome: origins and challenges. NeuroImage. 2013; 80:5361. [PubMed: 23528922].

[4] H. Zhang, A.J. Watrous, A. Patel, J. Jacobs (2018) Theta and Alpha Oscillations Are Traveling Waves in the Human Neocortex, Neuron, 98, 113, June 27, 2018 2018 Elsevier Inc. https://doi.org/10.1016/j.neuron.2018.05

[5] L. Muller, F. Chavane, J. Reynolds, T.J. Sejnowski (2018), Cortical travelling waves: mechanisms and computational principles. Nat Rev Neurosci. 2018 May ; 19(5): 255268. doi:10.1038/nrn.2018.20.

[6] A. Balossier, O. Etard, C. Descat, D. Vivien, E. Emery. 2016. Epidural cortical stimulation as a treatment for poststroke aphasia: a systematic review of the literature and underlying neurophysiological mechanisms. Neurorehabil Neural Repair, 30(2):120-30. doi: 10.1177/1545968315606989.

[7] N. Bessonov, A. Beuter, S. Trofimchuk, V. Volpert. (2018) Estimate of the travelling wave speed for an integro-differential equation. Applied Math Letters Applied Mathematics Letters, Volume 88, February 2019, Pages 103-110. https://doi.org/10.1016/j.aml.2018.07.037.

[8] N. Bessonov, A. Beuter, S. Trofimchuk, V. Volpert. Cortical waves and post-stroke brain stimulation. In press.

[9] A. Beuter, A. Balossier, S. Trofimchuk, V. Volpert. (2018) Modeling of post-stroke stimulation of cortical tissue. Mathematical Bioscience doi.org/10.1016/j.mbs.2018.08.014.

[10] G. Buzsaki, C.A. Anastassiou, C. Koch. The origin of extracellular fields and currents EEG, ECoG, LFP and spikes. Nat Rev Neurosci. ; 13(6) (2016), 407-420.

[11] B. Ermentrout, J.B. McLeod. Existence and uniqueness of travelling waves for a neural network. Proc. Roy. Soc. Edinburgh, 134A (1994), 1013-1022.

[12] Z. Chen, B. Ermentrout, X.J. Wang. Wave Propagation Mediated by GABAB Synapse and Rebound Excitation in an Inhibitory Network: A Reduced Model Approach. Journal of Computational Neuroscience 5 (1998), 53-69.

[13] J. Modolo, B. Bhattacharya, R. Edwards, J. Campagnaud, A. Legros, A. Beuter. Using a virtual cortical module implementing a neural field model to modulate brain rhythms in Parkinson's disease Frontiers in Neuroscience, 4 (2010), article 45.

[14] D.A. Pinotsis, E. Hansen, K.J. Friston, V.K. Jirsa. Anatomical connectivity and the resting state activity of large cortical networks Neuroimage, 65 (2013), 127-138.

[15] J. Senk, K. Korvasova, J. Schuecker, E. Hagen, T. Tetzlaff, M. Diesmann, M. Helias. Conditions for traveling waves in spiking neural networks. arXiv.org > q-bio > arXiv:1801.06046v1

[16] D.J. Pinto, G.B. Ermentrout. Spatially structured activity in synapticalaly coupled neuronal networks: I. Travelling fronts and pulses. SIAM J. Appl. Math., 62 (2001), No. 1, 206-225.

[17] D.J. Pinto, G.B. Ermentrout. Spatially structured activity in synapticalaly coupled neuronal networks: II. Lateral inhibition and standing pulses. SIAM J. Appl. Math., 62 (2001), No. 1, 226-243.

[18] F.M. Atay, A. Hutt. Neural Fields with Distributed Transmission Speeds and Long-Range Feedback Delays. SIAM J. Applied Dynamical Systems, 5 (2006), No. 4, 670-698.

[19] N.A. Venkov, S. Coombes, P.C. Matthews. Dynamic instabilities in scalar neural field equations with space-dependent delays. Physica D, 232 (2007), 1-15.

[20] G. Bard Ermentrout, Stefanos E. Folias, and Zachary P. Kilpatrick Spatiotemporal Pattern Formation in Neural Fields with Linear Adaptation, 119-151. In: S. Coombes et al. (eds.), Neural Fields, Springer-Verlag Berlin Heidelberg, 2014,

[21] W. Gerstner, W.M. Kistler, R.Naud, L. Paninski. Neuronal Dynamics. From single neurons to networks and models of cognition. Cambridge University Press, 2014.

[22] H.G.E. Meijer, S. Coombes. Travelling waves in a neural field model with refractoriness. J. Math. Biol., 68 (2014), 1249-1268.

[23] J. Pelt, A. van Ooyen. Estimating neuronal connectivity from axonal and dendritic density fields. Frontiers in Computational Neuroscience, 7 (2013), article 160.

[24] A. van Ooyen, A. Carnell, S. de Ridder, B. Tarigan, H.D. Mansvelder, F. Bijma, M. de Gunst, J. van Pelt. Independently Outgrowing Neurons and Geometry- Based Synapse Formation Produce Networks with Realistic Synaptic Connectivity. Plos One, 9 (2014), no. 1, e85858.

[25] H. R. Wilson, J. D. Cowan A Mathematical Theory of the Functional Dynamics of Cortical and Thalamic Nervous Tissue. Kybernetik, 80 (1973).

[26] J.Y. Wu, X. Huang, C. Zhang. Propagating Waves of Activity in the Neocortex: What They Are, What They Do. Neuroscientist. 2008 October ; 14(5): 487-502.

[27] J. Rapela (2018) Traveling waves appear and disappear in unison with produced speech. arXiv:1806.09559v1 [q-bio.NC] 25 Jun 2018.

[28] V. Botella-Soler, M. Valderrama, B. Crépon, V. Navarro, M. Le Van Quyen, (2012), Large-Scale Cortical Dynamics of Sleep Slow Waves. PLoS ONE 7(2): e30757. doi:10.1371/journal.pone.0030757.

[29] J. Gross, N. Hoogenboom, G. Thut, P. Schyns, S. Panzeri, et al. (2013) Speech Rhythms and Multiplexed Oscillatory Sensory Coding in the Human Brain. PLoS Biol 11(12): e1001752. doi:10.1371/journal.pbio.1001752.

[30] J. Weaver, (2013), How Brain Waves Help Us Make Sense of Speech. PLoS Biol 11(12): e1001753. doi:10.1371/journal.pbio.1001753.

[31] S. Sarubbo, A. De Benedictis, S. Merler, E. Mandonnet, S. Balbi, E. Granieri, H. Duffau, (2015), Towards a Functional Atlas of Human White Matter. Human Brain Mapping 00:0000 DOI: 10.1002/hbm.22832.

5 Appendix 1. Periodic waves in different models

Two equations with time delay. In the work [15] a single neuron population model (excitation)

$$\tau\frac{\partial u}{\partial t}=\int_{-\infty}^{\infty}P(x-y)\psi(u(y,t-d))du-u \tag{5.5}$$

and a two population model (excitation and inhibition)

$$\tau\frac{\partial u}{\partial t}=\int_{-\infty}^{\infty}\left(P_{11}(x-y)\psi_1(u(y,t-d))-P_{12}(x-y)\psi_2(v(y,t-d))\right)dy-u \tag{5.6}$$

$$\tau\frac{\partial v}{\partial t}=\int_{-\infty}^{\infty}\left(P_{21}(x-y)\psi_1(u(y,t-d))-P_{22}(x-y)\psi_2(v(y,t-d))\right)dy-v \tag{5.7}$$

are considered. Here $P(x)$ and $P_{ij}(x)$ are symmetric positive functions. A particular example of step-wise constant functions is studied. Periodic travelling waves cannot exist for the first model. They are observed for the second model. Existence of pulse solutions in a similar model without delay was studied in [17].

One equation with distributed speed and delay. Equation with a distributed propagation speed and time delay is considered in [18]:

$$L\left(\frac{\partial u}{\partial t}\right)=\alpha\int_0^{\infty}g(v)\int_{-\infty}^{\infty}K(z)S(u(x+z,t-|z|/v))dzdv+$$
$$\beta\int_0^{\infty}f(\tau)\int_{-\infty}^{\infty}F(z)S(u(x+z,t-\tau))dzd\tau, \tag{5.8}$$

where L is a second-order differential operator, the functions $K(z)$ and $F(z)$ include both activatory and inhibitory kernels. Different regimes are observed: periodic in time and independent of space, stationary periodic in space, periodic travelling waves.

The model with distributed time delay [19]

$$u(x,t)=\int_{-\infty}^{\infty}w(x-y)dy\int_{-\infty}^{t}\eta(t-s)f(u(y,s-|x-y|/v))ds.$$

The same regimes as above and oscillating Turing structures are observed.

Peer-reviewed version available at Mathematics 2020, 8, 1076; doi:10.3390/math8071076

Neural field model with linear adaptation. It is a two equation model

$$\tau \frac{\partial u}{\partial t} = -u - \beta v + \int_D w(x-y)F(u(y,t))dy, \tag{5.9}$$

$$\frac{1}{\alpha}\frac{\partial v}{\partial t} = u - v, \tag{5.10}$$

where the second variable represents a linear adaptation (see [20] and the references therein). A large variety of wave and patterns are observed including stationary periodic in space solutions, travelling waves, modulated travelling waves, stationary and oscillating bumps.

Neural field model with refractoriness. Periodic travelling waves are also found in one-equation model without inhibition term but with neuron refractoriness (time delay after firing) [22]:

$$\frac{1}{r}\frac{\partial u}{\partial t} = -u + \left(1 - \int_{t-1}^{t} u(x,s)ds\right) f(w \otimes u).$$

Here $\otimes$ denotes spatial convolution.

6 Appendix 2. The values of parameters

Periodic travelling waves behave as $\cos(\beta t + \xi x)$ with the time frequency β, space frequency ξ, and speed $c = -\beta/\xi$. With the interval length $L = 2$ cm, we get $\xi = 2\pi/L \approx 3$ cm^{-1}.

Let us consider the example of the simulations in Figure 4 with $\tau = 1$ and wave speed 0.3. If this value of τ corresponds to the characteristic time delay 10 ms ([18], [21] Chapter 2.3.1), that is time unit in the simulation corresponds to 0.01 s, then $c = 0.3 \times 100 = 30$ cm/s.

The time frequency $\beta = c\xi = 90$ s^{-1} belongs to the upper limit of the observed range. The value of the wave speed and, respectively, the time frequency linearly dependent on it can be decreased by the variation of parameters a_i and b_i.

Connectivity functions can be estimated from the data in [23, 24]. It exponentially decreases with the rate of decrease in the interval 3-10 times at the at the distance 0.03 cm. This corresponds to the exponential $\exp(-\mu x)$ with μ in the range $30 \div 40$ cm^{-1}.

Propagation speed measures vary depending of the methodology used. When macroscopic waves are recorded from EEG or from ECoG which have low spatial and high temporal resolutions, the propagation speeds varies between 1 and 10 meters/second. As indicated by Muller et al., [5] these results are compatible with the range of axonal conduction speeds of myelinated white matter fibres in the cortex. However, when measuring mesoscopic waves propagation speed using local field potential (LFP) from multielectrode arrays (MEAs) or from optical imaging signals recorded with voltage-sensitive dyes (VSDs) having high spatial

and temporal resolution, the propagation speeds varies from 0.1 to 0.8 metres per second, consistent with the axonal conduction speed of the unmyelinated long-range horizontal fibres within the superficial layers of the cortex as indicated by Muller et al. [5].